Evol Ecol (2014) 28:885–904
DOI 10.1007/s10682-014-9719-6

ORIGINAL PAPER

The shape of selection: using alternative fitness functions to test predictions for selection on flowering time

Arthur E. Weis · Susana M. Wadgymar · Michael Sekor · Steven J. Franks

Received: 21 January 2014 / Accepted: 13 June 2014 / Published online: 20 June 2014

Abstract Selection gradient analysis examines the strength and direction of phenotypic selection as well as the curvature of fitness functions, allowing predictions on and insights into the process of evolution in natural populations. However, traditional linear and quadratic selection analyses are not capable of detecting other features of fitness functions, such as asymmetry or thresholds, which may be relevant for understanding key aspects of selection on many traits. In these cases, additional analyses are needed to test specific hypotheses about fitness functions. In this study we used several approaches to analyze selection on a major life-history trait—flowering time—in the annual plant *Brassica rapa* subjected to experimentally abbreviated and lengthened growing seasons. We used a model that incorporated a tradeoff between the time allocated to growth versus the time allocated to reproduction in order to predict fitness function shape. The model predicted that optimal flowering time shifts to earlier and later dates as the growing season contracts and expands. It also showed the flowering time fitness function to be asymmetrical: reproductive output increases modestly between the earliest and the optimal flowering date, but then falls sharply with later dates, truncating in a 'tail of zeros'. Our experimental results strongly supported selection for early flowering in short season and selection for late flowering in long season conditions. We also found support for the predicted asymmetry of the flowering time fitness function, including a 'tail of zeros' at later flowering dates. The form of the fitness function revealed here has implications for interpreting estimates of selection on flowering time in natural populations and for refining predictions on evolutionary response

Electronic supplementary material The online version of this article (doi:10.1007/s10682-014-9719-6) contains supplementary material, which is available to authorized users.

A. E. Weis (✉)
Koffler Scientific Reserve at Jokers Hill, University of Toronto, Ontario L7B IK5, Canada
e-mail: arthur.weis@utoronto.ca

A. E. Weis · S. M. Wadgymar
Department of Ecology and Evolutionary Biology, University of Toronto, Ontario L7B IK5, Canada

M. Sekor · S. J. Franks
Department of Biology, Fordham University, 441 East Fordham Road, Bronx, NY 10458, USA

to climate change. More generally, this study illustrates the value of diverse statistical approaches to understanding mechanisms of natural selection.

Keywords Directional selection · Stabilizing selection · Non-linear selection · Fitness function · Fitness surface · Flowering time · *Brassica rapa*

Introduction

Natural selection occurs through a covariance between phenotype and fitness (Price 1970). Taking Price's insight a step further, Lande and Arnold integrated the fitness-phenotype covariance into a quantitative genetic framework through the development of selection gradient analysis, which links selection to evolutionary response through the breeder's equation (Lande 1979; Lande and Arnold 1983). This revolutionized the study of natural selection and launched thousands of studies on the intensity and direction of selection in natural populations (Kingsolver and Pfennig 2007). Discovering the *causes* of natural selection, however, requires additional tools (Mitchell-Olds and Shaw 1987; Wade and Kalisz 1990). Experimental manipulation of the environment and/or the phenotypic distribution can test hypotheses on selective agents, although manipulations are not often feasible.

In some cases selective mechanisms can be evaluated in further detail by a close examination of the fitness function (single trait) or fitness surface (multiple traits) shape. Some agents of selection shape fitness functions in predictable ways. Examples include sigmoid relationships between size and attack survival for seeds within fruits (Toju and Sota 2006) and gallmakers in their galls (Weis et al. 1985), as predicted from enemy/victim size ratios (see also Janzen and Stern 1998). In the case of plant defense against herbivores, optimality theory predicts an asymmetrical convex relationship between allocation to resistance and fitness, i.e., under-investing in defense by a certain amount has a more negative fitness effect than over-investing by the same amount (Simms and Rausher 1987; Mauricio and Rausher 1997; Franks et al. 2008). Mountford (1968) noted that with regard to increased litter size in mammals "the extra number at parturition is more than offset by the higher mortality between birth and weaning". With sibling competition for parental resources, the predicted fitness function for litter size rises slowly between the smallest and the optimal sizes, falls sharply with larger sizes, and truncates in a 'tail of zeros', i.e., litters so large that no offspring survives competition. The strength of selection on traits like these can be quantified through linear and quadratic selection gradients. However, when the predicted fitness function in neither a straight line nor a parabola, more comprehensive tests on selection mechanisms are achievable though alternative statistical models. As a case in point, we present an experimental study of selection on flowering time in an annual plant.

The scheduling of reproduction is among the most important life history traits (Stearns and Koella 1986; Kozlowski and Wiegert 1987). For plants, the timing for the seasonal transition from vegetative growth to flowering has a multitude of impacts on fitness, mediated through many agents, biotic and abiotic (Elzinga et al. 2007; Munguía-Rosas et al. 2011). The key determinant of selection considered by life history theory is the trade-off between the interval of time allocated to vegetative growth versus time allocated to mating and maturing seed (Cohen 1976; King and Roughgarden 1983; Ejsmond et al. 2010; Johansson et al. 2013). In annuals, the total time available is determined by the length of the growing season, which inevitably ends with death. Theory predicts that the longer a plant delays flowering, the longer it can grow at near-exponential rates, thereby

gaining an accelerating capacity to secure resources for reproduction. Too long a delay, however, limits the time it can use this capacity; a plant that first blooms the day before a killing frost may produce many flowers but will leave no viable offspring. If the season contracts or expands, the optimal flowering time advances or recedes.

Under the "time to grow-time to reproduce" trade-off, the flowering time fitness function should peak at later dates in long-season environments than in short ones (Fig. 1a), absent severe weather fluctuations across the season. In addition, the function is asymmetrical: the adverse consequences for starting "too late" will be stronger than for starting "too early." There will also be a truncation date separating earlier-flowering plants with some reproductive success from very late plants with zero success. These elements of fitness function shape cannot be detected through selection gradients.

This paper presents a model to generate predictions on the shape of a flowering time fitness function when it is estimated from a sample of plants drawn from a natural population. We then test these predictions through an experiment that varied the length of the growing season for California populations of *Brassica rapa.* These experiments are critical for testing the predictions for two reasons. First, they directly test the hypothesis that changing the growing season length causes a change in selection. Second, they extend our ability to examine the fitness function beyond the limits imposed by natural populations/environments. For example, if flowering "too late" were extremely costly, we would expect selection to have already removed late-flowering genotypes from a natural population, which then eliminates our ability to detect this cost. This cost can be revealed, however, by shortening the growing season: plants flowering at the optimal time for long season conditions may flower "too late" under early season conditions. We used selection gradient analysis to estimate the intensity and direction of selection in these experiments. To explore specific, model-based predictions on fitness function shape, we used three mutually reinforcing regression approaches, explained below.

Theoretical background

Theoretical treatments indicate that in seasonal environments, optimal flowering time covaries with the length of the growing season (e.g., Cohen 1976; King and Roughgarden 1983; Kozlowski 1992; Fox 1992; Ejsmond et al. 2010; Johansson et al. 2013). These models have aimed to find the optimal allocation of energy between the growth of vegetative (resource acquiring) structures and the development of reproductive structures. They predict that as the end of the growing season approaches, reproductive allocation should switch from zero to 100 % of daily photosynthetic assimilation. The longer the growing season, the later the allocation switch. A closer look at these models reveals an additional prediction: the flowering time fitness function is asymmetrical (Fig. 1), and plants that begin flowering past some late date are doomed to reproductive failure (Cohen 1976; King and Roughgarden 1983; Kozlowski 1992).

Regression is the obvious approach for comparing these predictions to real data. The challenge is to identify appropriate functional forms for regression. But before choosing regression functions, it is prudent to ask if the shape predicted from optimality models will be detectable in a fitness function estimated from a random sample of plants drawn from a heterogeneous population. Published plots showing the asymmetric relationship (e.g., King and Roughgarden 1983), depict numerical examples that vary flowering time while holding all other factors equal—factors such as growth rate and exact season length. But details of function shape can change with growth parameters, and a fitness function estimated from a

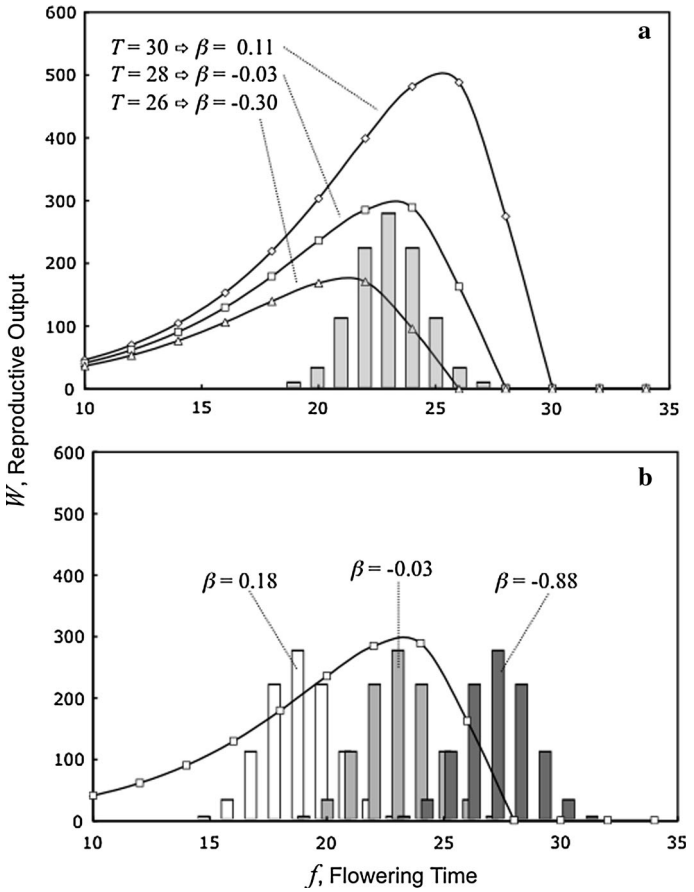

Fig. 1 Fitness functions for flowering time predicted by the modified logistic plant growth model. **a** Lines depict expected reproductive output for three different growing season lengths, T. The histogram represents a hypothetical phenotypic distribution of flowering times. The values of the univariate linear selection gradient, β, represent the intensity and direction of natural selection on flowering time in each of the growing season environments. Model parameter values: $g = 0.30$, $d = 0.002$. **b** Line depicts the fitness function in a single environment, while the three histograms represent three phenotypically distinct populations grown in that environment. The values of the univariate linear selection gradient, β, represent the intensity and direction of natural selection on flowering time for each population in this environment. Model parameter values: $g = 0.30$, $d = 0.002$, $T = 28$

variable population may or may not have the same features predicted from the 'all else equal' model. To sharpen our predictions we developed a model based on life-history theory, and then used it to see how fitness function shape may be manifest in a heterogeneous sample of plants.

Fitness function sensitivity to season length, and to growth and developmental rates

We modified a discrete-time model for plant vegetative growth (Weis and Hochberg 2000; Weis et al. 2000) that is based on the following logistic recursion equation:

$$V_{t+1} = V_t + \frac{gV_t}{1 + dV_t} - a_t V_t.$$

Here, V_t is the mass of vegetative tissues at time t, and g is the fundamental growth rate of the vegetative part. The d parameter determines the decline in realized growth rate as size increases, as would occur with self-shading and increased allocation to structural support. Thus the middle term on the right-hand side is the mass of assimilated resources that are then converted to new tissue during time interval t. The last term on the right-hand side is allocation to reproductive structures: during each time step, fraction a_t is invested in reproductive tissue. Reproductive output at time t is thus $R_t = a_t\ V_t$. Optimality models predict that over broad conditions, fitness is maximized when reproductive allocation is zero before flowering (i.e., when $t < f$). Once flowering starts ($t \geq f$), all current production is allocated to reproductive structures until the end of the season ($t = T$) (King and Roughgarden 1983; Kozlowski 1992). In our model this allocation pattern was achieved by making $a_t = g/(1 + dV_t)$ after flowering starts, but zero before. Lifetime reproductive output is

$$W = \sum_{t=f}^{T} R_t.$$

For simplicity we assume no herbivory or plant mortality before the end of the season, equal survivorship of seeds regardless of the date they are produced (see Ejsmond et al. 2010) and strong correlation between female and male fitness components.

To begin this exploration, we examine the relationship of f—time of first flowering—to reproductive output, W, in environments that differ in the length of the growing season, T. Figure 1a shows three realizations of the model with fixed values of g and d. These fitness functions exhibit the asymmetry of the optimality models, as well as the abrupt transition from non-zero to zero fitness beyond the critical date, T.

To see the implications of this fitness function shape, consider the direction and intensity of selection on a hypothetical population with a normal distribution of flowering times, but uniform in all other respects (Fig. 1a, histogram on x-axis). In this example the mean flowering time is at interval 23 (s.d. = 1.41). If exposed to an environment with a growing season of 28 intervals, the mean coincides with the optimal flowering time. Were the fitness function to be symmetrical, there would be no directional selection on flowering time. Instead, the asymmetry imposes weak, but non-zero directional selection for earlier flowering (univariate selection gradient, $\beta = -0.03$). If the growing season contracts by two intervals, selection for earlier flowering intensifies, but if it expands by two intervals, selection reverses direction. Note that in this example, the season contracts and expands by the same amount, but selection in the short season environment is almost 3 times stronger than in the late ($\beta = 0.30$ vs. 0.11, respectively). This difference in selection intensity can be attributed in part to the greater breadth of the fitness function with longer growing seasons, but the asymmetry of the function amplifies this effect.

The impact of asymmetry is more apparent in the example presented in Fig. 1b. Here we calculate the univariate selection gradient for three hypothetical plant populations, depicted as histograms upon the x-axis, for the $T = 28$ fitness function. The mean for the earliest-flowering population lies 4 intervals earlier than the optimal flowering time. It experiences moderate directional selection for later flowering times ($\beta = 0.18$). For the population flowering four intervals after the optimum, selection is in the opposite direction (for earlier flowering) and nearly five times stronger ($\beta = 0.88$).

Variations in g (fundamental growth rate), d (size-dependent decline in realized growth rate) and T (growing season length) effect the shape of the flowering time fitness function (Fig. 2a–c). Variation in growth rate causes divergence of the fitness functions at early flowering times, and weakly shifts the optima to later dates with lower growth rates (Fig. 2a). The functions converge on zero at the critical date, T. Change in the size-dependent growth rate parameter, d, has its strongest effect toward middle flowering times, and shifts the optimum to later times as it decreases (Fig. 2b). Low values of d may make the fitness function more leptokurtic. Individuals may also experience different growing season lengths: this can be due to micro-environment or variation in the time lag between flower production and seed maturation (see Cohen 1976; Kozlowski 1992). Variation in T strongly affects the optimum, causing fitness functions to diverge at later flowering dates (Fig. 2c). Despite differences in detail, the fitness functions retain the characteristic shape—asymmetry and truncation—as g, d and T are varied.

Making and testing predictions for heterogeneous populations

Our environmental manipulation experiment with *B. rapa* tested predictions on the shape of the flowering time fitness function. However, two more issues must be considered before testing empirically estimated functions against hypothesized shapes. First, natural populations are collections of individuals differing in growth and development rates. The fitness function shape predicted under the 'all else is equal' condition may be modified or lost in the noise of individual variation. Second, the range of flowering times in natural populations may be too narrow to reveal all of the potential features of fitness function shape (see Fig. 1).

Can we expect the flowering time fitness function to retain asymmetry and truncation when estimated from a heterogeneous population? Figure 3 illustrates a hypothetical mixed population, with the points taken from Fig. 2a–c. A locally weighted polynomial regression (see below) through the mean fitness for each flowering date (Fig. 3, solid curve) clearly shows the predicted asymmetry is evident in this heterogeneous population. The transition from non-zero to zero fitness at late flowering times is less abrupt, and resembles an asymptotic decline to zero, although zero is in fact achieved within the flowering time range. Neither of these two features is detectable from the quadratic regression fit to these data (Fig. 3, dashed curve).

The second issue arises because the shape of a function estimated over the narrow phenotypic range of a particular population may not show all of the features hypothesized for the broader range of potential flowering times (see Fig. 1b). The *B. rapa* populations used in this experiment differ in their mean and range of flowering times. Given model predictions and the limited range in observed flowering times, we expected three potential scenarios: (1) an asymmetrical, convex curve will best fit the relationship between flowering time and fitness when the fitness mode lies toward the center of the range: (2) if the fitness mode is later than the flowering time range, a decelerating upward trend is expected; and (3) if the fitness mode is earlier than the range, a downward, concave shape is expected, ending in a 'tail of zeros.' Given these expectations, the overall fitness function shape can be pieced together from fitness functions estimated for particular populations in particular seasonal environments.

Methods

We examined the relationship between flowering time and seed production for two *B. rapa* populations under long and short season treatments in the greenhouse. The data were

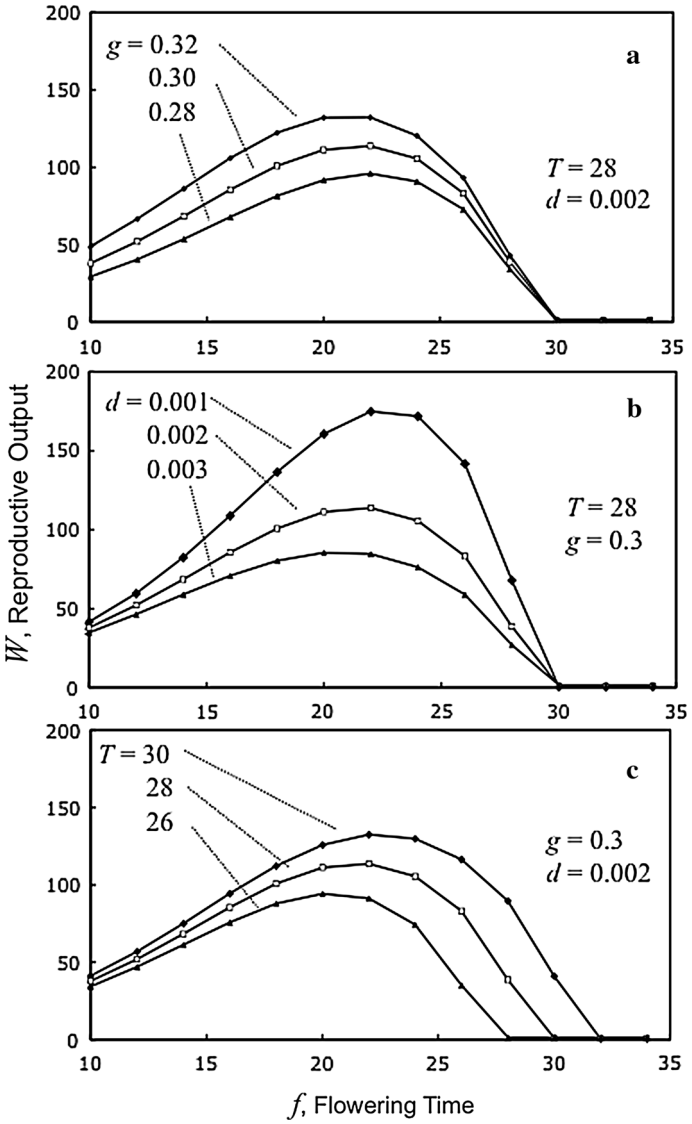

Fig. 2 Sensitivity of predicted fitness functions to variation in the growth model parameters. **a** Increasing basic growth rate, *g*, shifts function mode to earlier dates and causes functions to diverge over earlier flowering times. **b** Reducing the size-dependent deceleration in growth, *d*, shifts the function mode to later dates and causes functions to diverge over the mid-range of flowering times. **c** Extending the critical date for floral success, T, shifts the function mode to later dates and causes functions to diverge at later flowering times

collected during an experiment previously described by Franks et al. (2007) and Franks and Weis (2008), which can be consulted for further detail. One population (Back Bay) occupies a sandy bluff; its well-drained soil dries quickly, leading to an early summer drought in most years. The other population (Arboretum) grows on a low berm through a freshwater marsh; richer soil and a higher water table prolong its growing season by

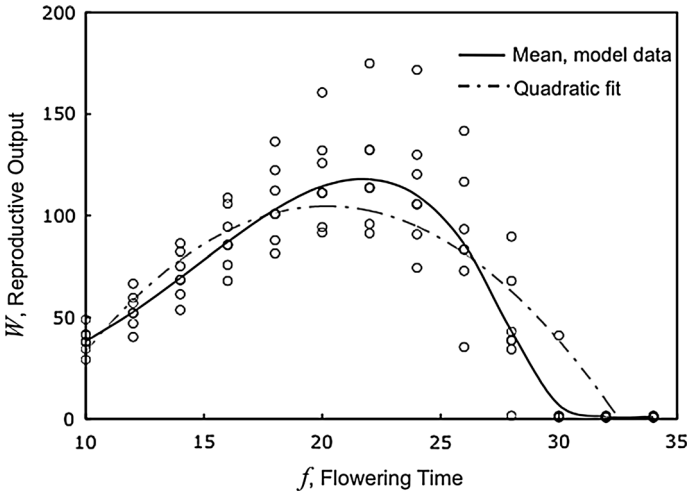

Fig. 3 The expected shape of the flowering time fitness function when estimated from a heterogeneous population. The points were taken form the model runs illustrated in Fig. 2. The *black curve* is the spline through the mean points at each flowering time, while the *dashed line* is the quadratic regression through all of the points

several weeks. Accordingly, mean flowering time for Back Bay is 10–12 days earlier than Arboretum (Fig. S1; see also Franke et al. 2006). Using a resurrection experiment, Franks et al. (2007) found that these *B. rapa* populations evolved a 2–8 day acceleration in flowering time over the course of a 5-year drought.

Experimental conditions

Plants were grown from seed derived from collections made in 1997 (ancestors) and 2004 (descendants). The field-collected seeds were used to grow a refresher generation that produced a crop of seeds maturing under uniform conditions, thus ameliorating maternal effects. F_1 hybrids between the ancestors and descendents were also produced during the refresher generation. We pooled the data for the three generations (1997, 2004 and hybrids) to expand the range in flowering time and thereby improve our ability to discern fitness function shape.

Growing season was manipulated through the watering regime. In the short season treatment, plants were watered at least once daily to saturation until day 51 after sowing. Pots were then allowed to dry gradually. The long season treatment was identical, except that watering continued until day 88. Watering treatment had a minor effect on flowering time (Table S1, Fig. S1). About 75 % of the plants had flowered at 51 days whereas all plants had flowered well before day 88. At senescence, we harvested and weighed all seeds in aggregate for every plant. Seed count per individual was estimated by regression. Seeds were counted for 20 plants in each population; more that 92 % of the variance in count was explained by weight.

Estimating selection gradients and fitting fitness functions

Linear and non-linear selection on flowering time was evaluated by selection gradient analysis (Lande and Arnold 1983; Stinchcombe et al. 2008). Seed count was relativized

(proportionate to the mean) and flowering time standardized to a zero mean and unit variance for each population-treatment separately. Many plants in the short season treatment produced zero seed, and so we used the aster package of R (Geyer et al. 2007; Shaw and Geyer 2010; R Development Core Team 2008) to estimate selection gradients, assuming a zero-inflated Poisson error distribution.

We assessed the shape of the fitness function though three alternative analyses: locally weighted polynomial regression, parametric non-linear regression, and piecewise regression.

Similar to the cubic spline (Schluter and Nychka 1994), the locally weighted polynomial regression produces a trend line by piecing together regression functions estimated for short, contiguous bands of the independent variable. Our analysis used a first order polynomial. Weights were assigned to observations within each band based on a Gaussian function of distance from the band mid-point. The shapes of the trend lines from such analyses are sensitive to the degree of smoothing applied; that is, how broad the bands are. Over-smoothed functions may not capture relevant patterns in the data, while under-smoothing can allow white noise to obscure important trends. We assessed the robustness of trend line features against smoothing with the graphical procedure called 'significant zero crossing of the derivatives' (SiZer) (Rondonotti et al. 2007; Sonderegger et al. 2009). SiZer evaluates the shape of the fitted curve through changes in the local slope. Specifically, the first derivatives of the locally weighted regressions are calculated at different degrees of smoothing, i.e., different band-widths. Confidence intervals for the derivative of the function at each value of the independent variable and at each band-width are calculated as per Hannig and Marron (2006). The SiZer method then graphically displays patterns of significance for local slope in a scale-space graph; in this case, flowering times are on the x-axis and the band-widths are arrayed along the y-axis. At a particular time/band-width combination, a significantly positive derivative (local slope positive) is represented by a dark grey block. Significantly negative derivatives (local slope negative) are shown in light grey. Derivatives that cannot be distinguished from zero signify no trend in the data and are illustrated in medium grey, while regions shown in white represent time/band-width combinations with insufficient data. SiZer graphs of the second derivative of the locally weighted polynomials highlight significant changes in curvature. Importantly, the SiZer graphical framework provides guidance for separating band-widths so narrow as to yield regressions that are uninformative because of under-smoothing, from band-widths so broad as to smooth-over statistically significant minima/maxima (and inflection points), i.e., band-widths that yield peaks and valleys in the locally weighted regression that demand explanation.

The second approach to analyzing the fitness function shape used maximum likelihood to fit parametric non-linear regression models to the data. Because the dependent variable was a count (number of seeds) a Poisson error distribution was assumed. We used different functional forms for the long and short season environments, as indicated by both theoretical expectations (Figs. 1, 2, 3) and by results of the SiZer analysis. In the short season environment, seed production appeared to fall as an exponential decay, and so data were fitted to the model,

$$W_i = \exp(a + mf_i) + e_i.$$

In the long season treatment, SiZer indicated a maximum that was internal to the data range. Given expectations of an asymmetrical function about this maximum, we employed the generalized epsilon-skew-normal (GESN) function. The basic ESN model is a mixture

of two half-normal distributions, with a skew parameter that determines the symmetry of the two halves (Hutson 2004). Clark and Thompson (2011) developed a generalized version of the model that can also account for kurtosis. The model is written as

$$W_i = \begin{cases} \exp\left[a + \left\{\dfrac{f-p}{b(1-s(1-p))}\right\}^k\right] & \text{for} \quad f \leq p \\ \exp\left[a + \left\{\dfrac{f-p}{b(1+s(1-p))}\right\}^k\right] & \text{for} \quad f > p \end{cases}$$

where a denotes the intercept, p the flowering time that achieves peak fitness, and b is the breadth of the function. When $s = 0$ and $k = 2$ (no skew or kurtosis) the model produces a normal curve. As s becomes more negative, the left tail of the curve is drawn out. Reducing k below 2 draws the curve into a sharper point while larger values flatten it. Clark and Thompson (2011), who provide R code for this procedure, illustrate the large variety of shapes that can be represented by varying s and k.

We used a hierarchical approach to assess the significance of the estimated skew and kurtosis coefficients. First, we fitted the data to the GESN function with s and k set to 0 and 2, respectively, i.e., a Gaussian curve. Then we compared the fit (-2 Log l) of the Gaussian curve to models estimating the two coefficients from the data. A significant improvement in fit, determined by χ^2, supports the skew and kurtosis hypotheses.

There are caveats in fitting the *B. rapa* data to the exponential decay and the GESN regression models. In one view, these functions can take the shapes expected in the two environments, but in another view they *impose* these shapes on the data. In a short season environment, for instance, we expect the fitness function to approach the 'tail of zeros' for later flowering times when individuals vary in the critical date for last flower, T. But if individuals are uniform for the critical date, an abrupt transition is expected. An exponential decay function will smooth over any abrupt transition, should it occur. Similarly, regression with the GESN function avoids the problem of imposing symmetry, but it can impose a peak on the data, even when one does not exist within the data range. For these reasons we employed a third approach.

We also fitted piecewise regressions to the fitness-flowering time data. This analysis uses maximum likelihood to fit regression coefficients on either side of an estimated breakpoint. Because of the Poisson error assumption the proper functional form for this analysis is the segmented exponential decay, rather than linear:

$$W_i = \begin{cases} \exp[a + mf_i] + e_i & \text{for} \quad f \leq v \\ \exp[a + mf_i + \Delta m(f_i - v)] + e_i & \text{for} \quad f > v \end{cases}$$

where v is the breakpoint between curve segments. The 'slope' coefficient for the left segment is denoted by m while Δm denotes the *change* in the coefficient across the break point (Toms and Lesperance 2003). Thus, a Δm significantly different from zero implies that the right-hand segment shows a different decay rate than the left. Rather than report Δm, we report the left- and right-hand coefficients (m_L and m_R) $\pm$ standard error, for a more concrete representation of the fitness function shape. Piecewise models can be expanded to accommodate multiple breakpoints and segments, which we did where the SiZer analysis indicated. A sharp threshold for transition from non-zero to zero fitness would be evidenced by a significantly negative coefficient for the penultimate segment, followed by a zero decay coefficient for the final segment. This method can also test for a fitness peak internal to the data, which is evidenced by a significantly positive coefficient

Table 1 Selection gradient estimates for flowering time for both populations in both season length treatments

Selection gradient	Back bay				Arboretum			
	Raw data		Aster estimated		Raw data		Aster estimated	
	Estimate	(SE)	Estimate	(SE)	Estimate	(SE)	Estimate	(SE)
Short season								
Linear (ß)	**−0.387**	(0.058)	**−0.384**	(0.011)	−0.196	(0.092)	**−0.197**	(0.001)
Quadratic (γ)	**0.064**	(0.020)	**0.056**	(0.002)	0.049	(0.065)	**−0.007**	(0.0006)
Long season								
Linear (ß)	**0.102**	(0.029)	**0.102**	(0.004)	**−0.027**	(0.031)	**−0.027**	(0.003)
Quadratic (γ)	−0.050	(0.018)	**−0.007**	(0.002)	**−0.133**	(0.025)	**−0.032**	(0.002)

'Raw Data' gradients were calculated directly from observed values using the Lande and Arnold (1983) approach, while 'Aster Estimated' gradients were calculated using fitness estimates from the *Aster* procedure (Geyer et al. 2007). Bold coefficients are significantly different from zero at or beyond $P = 0.002$ level

rising to a breakpoint, followed by a significantly negative coefficient in the subsequent segment—an inverted "V". Asymmetry in the fitness-flowering time relationship is revealed by a *z*-test for the absolute values for segment coefficients. When Δm is not significantly different from zero at any value of v, the data are better described by a simple exponential decay.

All analyses were made using R (R Development Core Team 2008). The non-parametric analyses were performed with the SiZer package (Sonderegger 2011) in R 2.15.0. The exponential decay and GESN function were fitted with the `bbmle` package (Bolker and Team 2011) and the piecewise regression was performed with the `segmented` package (Muggeo 2008). Although we assumed a Poisson error distribution, mean seed count was sufficiently large (ranging from 87 to 1138, depending on population and environment) that errors could approach a normal distribution. The analyses were repeated assuming a normal error distribution and are presented in the Supplementary Information. In these analyses, linear functions were used in the segmented regression. Results were substantially the same for both sets of analyses.

Results

Selection and fitness functions in the short season environment

As predicted, directional selection favored earlier flowering time in the short growing season treatment. Directional selection gradients in both the Lande and Arnold, and the aster analysis approaches were significantly negative (Table 1). The positive quadratic selection gradients suggest an overall concave curvature to the fitness function. The non-parametric regressions produced concave, downward trend curves in fitness with increasing flowering times in both populations (Fig. 4a, d).

In the early-flowering Back Bay population, SiZer analysis shows that even at narrow band-widths the non-parametric regression was significantly downward over early flowering times, and indistinguishable from zero at late flowering times (Fig. 4b). As bandwidth increases, the negative trend extends to later flowering times, but a zero trend

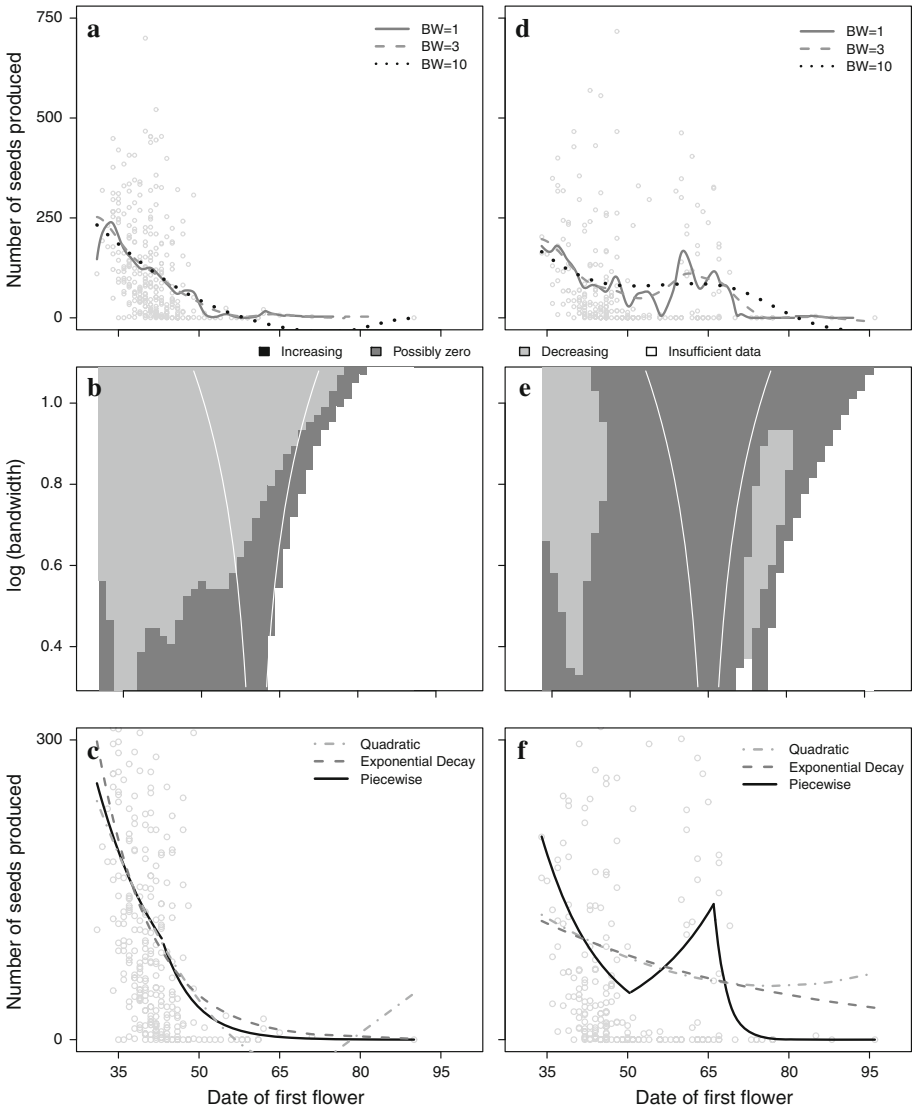

Fig. 4 Estimated fitness functions for the Back Bay (**a**–**c**) and Arboretum (**d**–**f**) populations of *Brassica rapa* in the short season environment. **a**, **d** Locally weighted polynomial regressions at three band-widths (levels of smoothing). **b**, **e** SiZer analysis graphs showing the sign of the first derivatives of locally weighted polynomial regression, evaluated at the observed flowering times, over a range of band-widths. *Dark grey* regions indicate significantly positive slope to the first derivative, *light grey* indicates a negative slope while slopes in the medium grey regions are indistinguishable from zero. *White regions* indicate insufficient data for analysis. The diverging curves though the center of the space illustrate band-width size at each horizontal slice though the space. **c**, **f** Fitted regression models to the data. The *dashed grey line* plots the regular exponential decay function, while the *solid black line* is the segmented exponential decay model. Note the range on the *y*-axis is constricted to facilitate comparison among the fitted functions. Parameter estimates and their standard errors are given in Table 2. The quadratic regression is plotted in *light grey* for reference

Table 2 Parameter estimates for fitness functions in the short season environment

Parameter	Back bay		Arboretum	
	Estimate	(SE)	Estimate	(SE)
Exponential decay				
a	8.81	(0.512)	5.50	(0.036)
m	−0.10	(0.001)	−0.02	(0.001)
	AIC = 31,833		AIC = 38,318	
Piecewise linear				
a	8.11	(0.070)	8.370	(0.086)
m_L	−0.08	(0.002)	−0.090	(0.002)
m_C	–	–	0.158	(0.004)
m_R	−0.10	(0.007)	−0.503	(0.027)
v_1	44.30	(0.272)	50.370	(0.247)
v_2	–	–	66.010	(0.115)
	AIC = 31,529		AIC = 35,064	

All parameter estimates were significantly different from zero beyond the $P = 0.001$ level

remains at the latest time. The SiZer graph of the second derivative of the non-parametric regression (Fig. S2) indicates that the rate of decline decreases between the earliest and middle flowering dates (concave curvature), but no change in rate of decline for later dates (plateau).

The exponential decay regression (Fig. 4c; Table 2) indicated an asymptotic decline to zero fitness at later flowering times. However, the SiZer graph suggested a potential breakpoint beyond which seed count levels out at zero. The piecewise exponential regression detected a significantly negative left-hand coefficient up to day 44 (Fig. 2c). Although we expected a near-zero coefficient beyond the break point, the right-hand coefficient was more negative (Table 2). Comparing coefficients of the two parametric regression approaches (Table 2) shows that the piecewise procedure detected a weaker decline in fitness with flowering up to a breakpoint than seen in the simple exponential procedure, but the same rate of decline thereafter. The AIC value was smaller for the piecewise analysis (Table 2), but the prediction curves of the regular and piecewise functions were quite similar to one another (Fig. 4c) and to the non-parametric trend lines (Fig. 4a). All are different from the quadratic relationship, plotted for reference in Fig. 4c.

The fitness function of the later-flowering Arboretum population was generally similar to Back Bay, except in one respect. SiZer analysis revealed a significant downward trend in the fitness function at early flowering times at all band-widths (Fig. 4d, e). A second, narrower range for a downward fitness trend was detected at later flowering times, but only at low to medium band-widths. The exponential decay regression function supported a weak loss of fitness with increasing flowering times for the Arboretum population (Fig. 4e; Table 2), but this function is uninformative about the more complex shape suggested by the non-parametric regression. The piecewise regression, however, did indicate a more complex shape (Fig. 4e). This analysis estimated breakpoints at days 46 and 66. The left-hand segment had a negative coefficient, as expected, while the center segment had a positive one. The right-hand segment had a very steep negative coefficient, which indicates a strong exponential decay to zero. The 3-segmented fit for the Arboretum population

under the short growing season is the results of an appreciable number of plants with intermediate flowering times achieving high seed production.

Selection and fitness functions in the long season environment

The Lande and Arnold and the aster analysis approaches showed that in the long season treatment, there was strong selection for later flowering in the Back Bay population and very weak selection for earlier flowering in the Arboretum population (Table 1). These results fit predictions and are biologically reasonable: the Back Bay population has an early mean flowering time, so should be under stronger selection to flower later under long season conditions. The Arboretum population has a later mean flowering time, so may already be close to the supposed optimal flowering time under the long season conditions. Negative quadratic selection gradients suggest overall convex curvature for the fitness functions, consistent with stabilizing selection. Again this seems reasonable since we expect an intermediate optimum flowering time under long season conditions.

Similar to the selection gradient analysis, non-parametric regression suggested selection for delayed flowering for the Back Bay population in the long season (Fig. 5a). Specifically, this approach showed a strong increase in fitness with flowering time over the earlier end of the observed range of data, but little change in fitness across the later end of the range (Fig. 5a). SiZer analysis confirms this: between days $\sim$40 and 50 the first derivatives transition from positive to near-zero values (Fig. 5b) while second derivatives indicate convex curvature (Fig. S2). In the GESN analysis (Table 3; Fig. 5c), the larger breadth coefficient, b, combined with a positive skew coefficient, s, confirms that the rise to the predicted fitness peak is far steeper than any decline at later flowering times. In contrast to the SiZer analysis, the GESN fit produced convex curvature over early flowering times ($k < 2$). Although GESN fitted a peak internal to the data range, the piecewise regression provides weaker support for this (Fig. 5c, Table 3); the left-hand coefficient is positive, but the right-hand coefficient is very nearly zero. Despite the disagreements in detail among the three regression approaches, all three support the notion that when an early-flowering population inhabits a long season environment, fitness increases with flowering time over the lower end of the range. The date for peak fitness predicted by the quadratic function (plotted for comparison in Fig. 5c) is over 10 days later than those indicated by the GESN and segmented functions.

A strong component of stabilizing selection is evident for the later-flowering Arboretum population under the long season environment (Fig. 5d–f). SiZer analysis of the non-parametric regressions showed a downward trend in fitness over flowering times longer than $\sim$62 days across all band-widths, and an upward trend over earlier flowering time at higher band-widths (Fig. 5e). Both the GESN and piecewise regressions indicate a peak at day 61 (Table 3; Fig. 5f). Both regressions also detected the predicted asymmetry. This is evidenced by the significantly negative skew parameter for the GESN regression and by the significantly greater absolute value of the right-hand coefficient ($z = 73$, $P < 0.0001$) in the piecewise regression (Table 3; Fig. 5f). Further, the fitness function is leptokurtic, as evidenced by the low value of k, and the significantly positive second derivatives at early flowering times (Table S3). We note that although the mean flowering time in the population and treatment ($\bar{f} = 54.5$ days) precedes the fitness peak ($p \approx 61$ days), there is still a weak downward selection gradient on flowering time (Table 1), which can be attributed to the asymmetry of the fitness function.

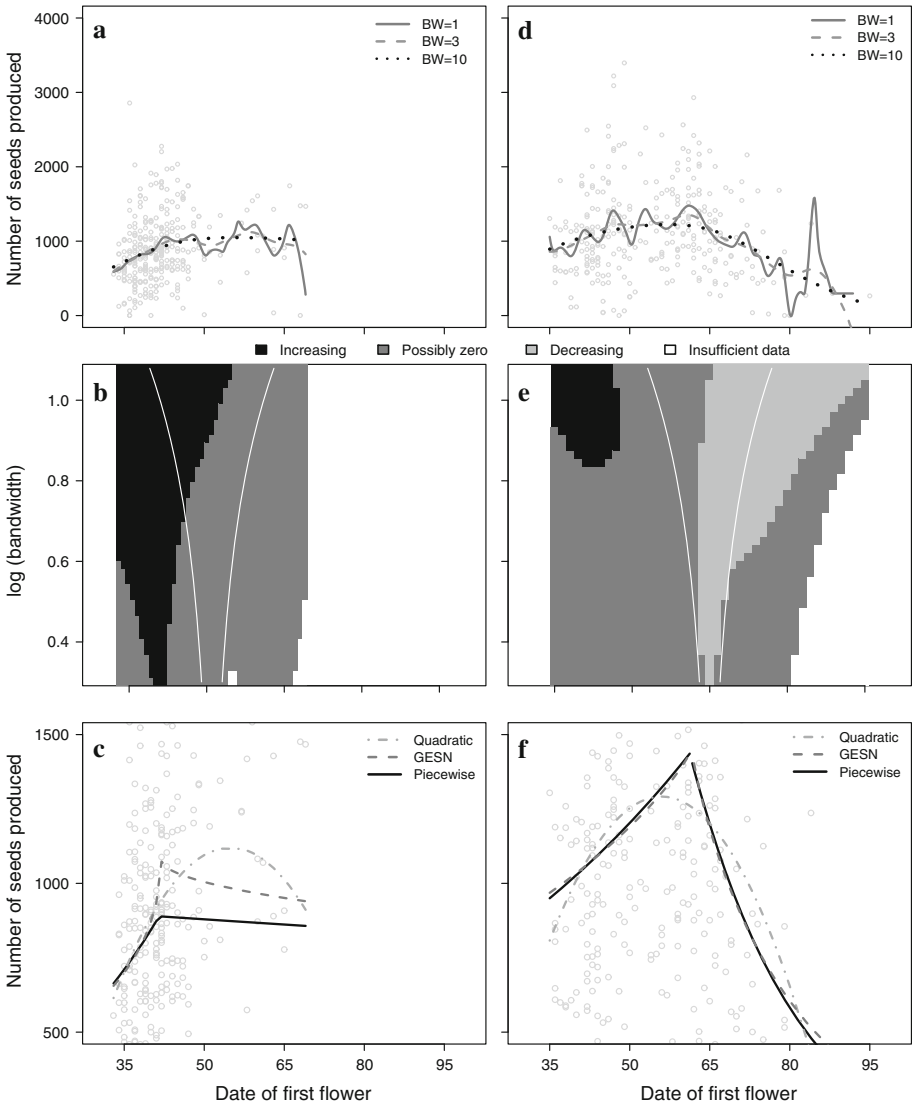

Fig. 5 Estimated fitness functions for the Back Bay (**a**–**c**) and Arboretum (**d**–**f**) populations of *Brassica rapa* in the long season environment. Panels **a**, **b**, **d** and e as in Fig. 4. Panels **c** and **f** plot the fitted generalized epsilon-skew-normal (*dashed*, *dark grey*) and the segmented exponential (*solid*, *black*) functions. Note the range on the *y*-axis is constricted to facilitate comparison among the fitted functions. Parameter estimates and their standard errors are given in Table 3. The quadratic regression is plotted in *light grey* for reference

Discussion

Growing evidence suggests that flowering time can rapidly evolve in response to changing climatic conditions (Franks et al. 2013) and as invasive species expand their ranges (Dlugosch and Parker 2008; Colautti and Barrett 2013). In one such study we found that

Table 3 Parameter estimates for fitness functions in the long season environment

Parameter	Back bay		Arboretum	
	Estimate	(SE)	Estimate	(SE)
Generalized epsilon-skew-normal				
a	**6.98**	(0.005)	**7.28**	(0.006)
p	**41.99**	(0.002)	**61.63**	(0.095)
b	**486.02**	(40.15)	**48.87**	(1.209)
s	**0.94**	(0.004)	**−0.561**	(0.117)
k	**0.57**	(0.019)	**0.86**	(0.025)
	AIC = 71,715		AIC = 91,016	
Piecewise linear				
a	**5.366**	(0.0511)	**6.309**	(0.0014)
m_L	**0.034**	(0.0013)	**0.016**	(0.0003)
m_R	**−0.001**	(0.0004)	**−0.064**	(0.0007)
v	**43.25**	(0.1171)	**61.250**	(0.0969)
	AIC = 71,471		AIC = 91,035	

Estimates indicated in bold are nominally different from null expectation at the 0.05 significance level

our California *B. rapa* populations evolved a 2–8 day acceleration in flowering time over the course of a 5-year drought. That experiment eliminated phenotypic plasticity as a source of flowering time change: ancestral, pre-drought generations (resurrected from stored seed) were grown in a common garden simultaneously with their post-drought descendents (Franks et al. 2007). The mean flowering times of the two generations diverged. F_1 hybrids from crosses between ancestors and descendents showed intermediate flowering times, confirming an additive genetic basis for the divergence. Since the extended drought shortened the rainy/growing season for five consecutive generations (Franks et al. 2007), we posited that the evolutionary change was due to directional selection for early flowering time that came with the shift from long to short growing seasons. The present study confirms that a growing season shortened by drought does indeed cause selection for early flowering. It also shows that extending the growing season by continued watering reverses the direction of selection.

Other factors may impose selection on flowering time. Within-season climate trends together with the wax and wane of pollinators and/or seed predators will change environmental quality over the course of the population's flowering period (Pettersson 1994; Pilson 2000; Elzinga et al. 2007; Forrest and Thomson 2011). A plant's flowering time thus determines which segment of this temporally shifting environment it occupies, which in turn impacts its fitness. The greenhouse environment for this experiment was probably less variable over time than the natural habitats for our populations, and so the impact of the 'time to grow-time to reproduce' tradeoff on selection could be stronger here than in the wild. By the same token, these experimental conditions increase our confidence that the fitness functions we estimated were primarily shaped by the impact of growing season length.

Selection gradient analysis (Lande and Arnold 1983) was sufficient to test the basic prediction about the change in the direction and intensity of selection with change in the growing season length. Aster analysis was particularly useful in estimating the selection gradients in the short season environment, given the large number of plants with zero seed

counts. Selection gradient analysis performed on the aster-estimated values produced linear selection gradients virtually identical to those produced by selection gradient analysis on the raw fitness values. Due to the simplicity of the aster model (based a single trait in an annual life cycle) the selection gradient analysis using aster yielded smaller standard errors and conflicting quadratic selection gradients. Regardless, additional statistical tools were needed to test the more nuanced predictions about the shape of the fitness function.

Models that posit a trade-off between time allocated to vegetative growth and time allocated to reproduction predict a greater fitness penalty for flowering too late than for flowering too early. Plants that flower after some critical date die at season's end without producing viable offspring. The California populations did not provide a sufficient range of phenotypes to span all features of the hypothesized fitness function in any one environment, but the overall shape of selection can be pieced together from the four population-environment combinations, with each combination exhibiting a segment of a broader fitness function (see Fig. 1b). To review, we expected: (1) an asymmetrical, convex curve when the fitness mode lies toward the center of the phenotypic range: (2) a decelerating upward trend in fitness when the upper end of the phenotypic range lies to the left of the fitness function peak; and (3) a downward concave shape, ending in a 'tail of zeros' when the lower end of the range lies to the right of the peak.

Expectation 1 was met for the Arboretum population in the long season environment. All three of the regression analyses indicated that fitness was maximized by flowering at $\sim$61 days, which was well within the observed range in flowering times. Evidence for asymmetry included a significantly negative skew coefficient in the GESN regression, and in the piecewise regression, by a right-hand downward coefficient that was significantly steeper than the upward left-hand one. This makes biological sense. Plants that flower early, flower at a small size and so have a low daily offspring production rate. But early plants can partially compensate for the low daily rate by reproducing for more days. Plants that flower late have a greater daily offspring production rate, but die before they can fully capitalize on this capacity.

The Back Bay population had an earlier mean and a narrower range for flowering time. As a result, evidence for a peaked fitness function in the long season is weak for this population. The GESN regression imposes a peak at day 41 on these data, and in so doing, fits a positive skew coefficient. However, the segmented regression model suggest a breakpoint at day 43, with an essentially zero-slope line through the few points beyond this date. Combined with the SiZer analysis of the non-parametric regression, these results are somewhat consistent with expectation 2, i.e., a decelerating increase in fitness with flowering time. Plants at the high end of the flowering time range in this population were presumably near the point where the time spent amassing reproductive capacity was balanced by the time spent using it.

Expectation 3—a convex decrease in fitness to a 'tail of zeros' when the data range is past the fitness mode—is strongly supported by the Back Bay population in the short season environment. By withholding water early in the experiment, the peak of the fitness function should move to a very early date. Both the SiZer analysis and the exponential decay regression indicate a negative trend in fitness that flattens to essentially zero at late flowering times. Plants that flowered early in this situation had limited time for reproduction, while those that flowered late had none. Note that the average seed count for plants in the short season was one-fifth of those in the long season environment, giving further evidence for a time limitation. Although the segmented regression found a statistically significant evidence for a break point, this did not correspond to an abrupt transition from non-zero to zero fitness as predicted from flowering time models, where plants are

identical for all features except flowering time (see Fig. 1). Rather, it more resembled the smooth decline to zero expected for heterogeneous populations (see Fig. 3). Support for expectation 3 in the Arboretum was complicated by a large number of intermediate flowering individuals that achieved unexpectedly high seed production. This led to a three-segmented fit to the data. Nevertheless, the final segment showed clear signs of a decline to zero fitness at the latest flowering times.

Taken together, these analyses present a coherent picture of the shape of selection on flowering time, as imposed by growing season length. They support the basic prediction that the optimal flowering time shifts as the growing season expands or contracts. They further illustrate how the intensity of selection on a trait depends on the position of the phenotypic range along the underlying fitness function. The shape of the underlying fitness function detected here has an interesting property: the population comes to a selective equilibrium (i.e., selection is purely stabilizing) when the population mean reaches a value that is earlier than the optimal time (see also, Mountford 1968).

There is an interesting implication of the asymmetric fitness function for the evolution of flowering time in response to climate change. In regions where the season is shortened, species should show a faster evolutionary response than those in regions where the season is extended. For instance, all else equal, an abbreviated rainy season in a Mediterranean zone may occasion rapid evolution of early flowering, while the evolution of delayed flowering would occur more slowly in a warming boreal environment, even when the absolute value of the shift in optimal flowering time is the same.

The modeling, experimentation and analyses we presented here illustrate what we think is a fruitful approach to understanding mechanisms generating natural selection. When a theoretical model predicts a specific type of relationship between phenotype and fitness, those predictions can be tested by fitting experimental data to alternative regression functions. We also would suggest that applying a broader array of regression models to data from natural populations could be useful for generating new hypotheses on selection mechanisms. The particular procedures used in the present case may or may not have wide application, and there may be even better procedures for analyzing this experiment. The point is that while selection gradient analysis detects the direction and intensity of selection, there are many important questions on the causes of selection that can be addressed only through other means.

Acknowledgments We thank K. Afshar, V. Chandrasekaran, A. Dick, A. Franks, L. Gonzalez, C. Herman, L. Hua, E. Ko, T. Kossler, P. Le, K. Musser, A. Ng, M. Ngugen, A. Ogura, P. Rath, S. Sim, K. Torosian, P. Tran, W. Yang, A. M. Weis, A. N. Weis and E. Weiss for greenhouse assistance. Denise Franke made the 1997 seed collections. Ruth Shaw and Charles Geyer advised us on the aster analyses. Emily Austen, Jennifer Ison and Russell Lande offered valuable comments on earlier drafts and Jean Weis assisted with proofreading. Thanks go to Nancy and Tom Dier for providing AEW with a convivial place to write. Support came from grants by the National Science Foundation (DEB-0345030) and from the National Science and Engineering Research Council to AEW. SJF was supported by a grant from the National Science Foundation (DEB-1142784).

References

Bolker B, R Development Core Team (2011) bbmle: tools for general maximum likelihood estimation. R package version 1.0. 4.1

Clark RM, Thompson R (2011) Estimation and comparison of flowering curves. Plant Ecol Divers 4:189–200

Cohen D (1976) The optimal timing of reproduction. Am Natur 110:801–807

Colautti RI, Barrett SCH (2013) Rapid adaptation to climate facilitates range expansion of an invasive plant. Science 342:364–366
Dlugosch KM, Parker IM (2008) Founding events in species invasions: genetic variation, adaptive evolution, and the role of multiple introductions. Molec Ecol 17:431–449
Ejsmond MJ, Czarnoleski M, Kapustka F, Kozlowski J (2010) How to time growth and reproduction during the vegetative season: an evolutionary choice for indeterminate growers in seasonal environments. Am Natur 175:551–563
Elzinga JA, Atlan A, Biere A, Gigord L, Weis AE, Bernasconi G (2007) Time after time: flowering phenology and biotic interactions. Trends Ecol Evol 22:432–439
Forrest JR, Thomson JD (2011) An examination of synchrony between insect emergence and flowering in Rocky Mountain meadows. Ecol Monogr 81:469–491
Fox GA (1992) Annual plant life histories and the paradigm of resource allocation. Evol Ecol 6:482–499
Franke DM, Ellis AG, Dharjwa M, Freshwater M, Fujikawa M, Padron A, Weis AE (2006) A Steep cline in flowering time for *Brassica rapa* in southern California: population-level variation in the field and the greenhouse. Int J Plant Sci 167:83–92
Franks SJ, Weis AE (2008) A change in climate causes rapid evolution of multiple life-history traits and their interactions in an annual plant. J Evol Biol 21:1321–1334
Franks SJ, Sim S, Weis AE (2007) Rapid evolution of flowering time by an annual plant in response to a climate fluctuation. PNAS 104:1278–1282
Franks SJ, Pratt PD, Dray FA, Simms EL (2008) Selection on herbivory resistance and growth rate in an invasive plant. Am Natur 171:678–691
Franks SJ, Weber JJ, Aitken SN (2013) Evolutionary and plastic responses to climate change in terrestrial plant populations. Evol Appl 7:123–139
Geyer CJ, Wagenius S, Shaw RG (2007) Aster models for life history analysis. Biometrika 94:415–426
Hannig J, Marron JS (2006) Advanced distribution theory for SiZer. J Am Stat Assoc 101:484–499
Hutson A (2004) Utilizing the flexibility of the epsilon-skew-normal distribution for common regression problems. J Appl Stats 31:673–683
Janzen FJ, Stern HS (1998) Logistic regression for empirical studies of multivariate selection. Evolution 52:1564–1571
Johansson J, Bolmgren K, Jonzén N (2013) Climate change and the optimal flowering time of annual plants in seasonal environments. Global Change Biol 19:197–207
King D, Roughgarden J (1983) Energy allocation patterns of the California grassland annuals *Plantago erecta* and *Clarkia rubicunda*. Ecology 64:16–24
Kingsolver JG, Pfennig DW (2007) Patterns and power of phenotypic selection in nature. Bioscience 57:561–572
Kozłowski J (1992) Optimal allocation of resources to growth and reproduction: implications for age and size at maturity. Trends Ecol Evol 7:15–19
Kozłowski J, Wiegert RG (1987) Optimal age and size at maturity in annuals and perennials with determinate growth. Evol Ecol 1:231–244
Lande R (1979) Quantitative genetic analysis of multivariate evolution, applied to brain: body size allometry. Evolution 33:402–416
Lande R, Arnold SJ (1983) The measurement of selection on correlated characters. Evolution 37:1210–1226
Mauricio R, Rausher MD (1997) Experimental manipulation of putative selective agents provides evidence for the role of natural enemies in the evolution of plant defense. Evolution 51:1435–1444
Mitchell-Olds T, Shaw RG (1987) Regression analysis of natural selection: statistical inference and biological interpretation. Evolution 41:1149–1161
Mountford MD (1968) The significance of litter-size. J Anim Ecol 37:363–367
Muggeo VM (2008) Segmented: an R package to fit regression models with broken-line relationships. R News 8:20–25
Munguía-Rosas MA, Ollerton J, Parra-Tabla V, De-Nova JA (2011) Meta-analysis of phenotypic selection on flowering phenology suggests that early flowering plants are favoured. Ecol Lett 14:511–521
Pettersson MW (1994) Large plant size counteracts early seed predation during the extended flowering season of a *Silene uniflora* (Caryophyllaceae) population. Ecography 17:264–271
Pilson D (2000) Herbivory and natural selection on flowering phenology in wild sunflower, *Helianthus annuus*. Oecologia 122:72–82
Price GR (1970) Selection and covariance. Nature 227:520–521
R Development Core Team (2008) R: a language and environment for statistical computing. R Foundation for Statistical Computing, Vienna, Austria. ISBN 3-900051-07-0. http://www.R-project.org
Rondonotti V, Marron JS, Park C (2007) SiZer for time series: a new approach to the analysis of trends. Elec J Stats 1:268–289

Schluter D, Nychka D (1994) Exploring fitness surfaces. Am Natur 143:597–616
Shaw RG, Geyer CJ (2010) Inferring fitness landscapes. Evolution 64:2510–2520
Simms EL, Rausher MD (1987) Costs and benefits of plant resistance to herbivory. Am Natur 130:570–581
Sonderegger D (2011) SiZer: significant zero crossings. R package version 0.1–4
Sonderegger DL, Wang H, Clements WH, Noon BR (2009) Using SiZer to detect thresholds in ecological data. Front Ecol Environ 7:190–195
Stearns SC, Koella JC (1986) The evolution of phenotypic plasticity in life-history traits: predictions of reaction norms for age and size at maturity. Evolution 40:893–913
Stinchcombe JR, Agrawal AF, Hohenlohe PA, Arnold SJ, Blows MW (2008) Estimating nonlinear selection gradients using quadratic regression coefficients: double or nothing? Evolution 62:2435–2440
Toju H, Sota T (2006) Imbalance of predator and prey armament: geographic clines in phenotypic interface and natural selection. Am Natur 167:105–117
Toms JD, Lesperance ML (2003) Piecewise regression: a tool for identifying ecological thresholds. Ecology 84:2034–2041
Wade MJ, Kalisz S (1990) The causes of natural selection. Evolution 44:1947–1955
Weis AE, Hochberg ME (2000) The diverse effects of intraspecific competition on the selective advantage to resistance: a model and its predictions. Am Natur 156:276–292
Weis AE, Abrahamson WG, McCrea KD (1985) Host gall size and oviposition success by the parasitoid *Eurytoma gigantea*. Ecol Entom 10:341–348
Weis AE, Simms EL, Hochberg ME (2000) Will plant vigor and tolerance be genetically correlated? Effects of intrinsic growth rate and self-limitation on regrowth. Evol Ecol 14:331–352